AGU PUBLICATIONS

JGR

Journal of Geophysical Research: Space Physics

RESEARCH ARTICLE

10.1002/2014JA020457

Key Points:
- The EMP from lightning has a stronger effect in gaseous planets than on Earth
- The EMP creates ionization and light upper atmosphere of Saturn and Jupiter
- Light emitted by the EMP is one tenth of the light from the lightning stroke

Supporting Information:
- Readme
- Figure S1
- Figure S2
- Text S1

Correspondence to:
A. Luque,
aluque@iaa.es

Citation:
Luque, A., D. Dubrovin, F. J. Gordillo-Vázquez, U. Ebert, F. C. Parra-Rojas, Y. Yair, and C. Price (2014), Coupling between atmospheric layers in gaseous giant planets due to lightning-generated electromagnetic pulses, *J. Geophys. Res. Space Physics*, *119*, 8705–8720, doi:10.1002/2014JA020457.

Received 1 AUG 2014
Accepted 7 OCT 2014
Accepted article online 12 OCT 2014
Published online 30 OCT 2014

Coupling between atmospheric layers in gaseous giant planets due to lightning-generated electromagnetic pulses

A. Luque[1], D. Dubrovin[2], F. J. Gordillo-Vázquez[1], U. Ebert[3], F. C. Parra-Rojas[1], Y. Yair[4], and C. Price[2]

[1]Institute for Astrophysics of Andalusia, Granada, Spain, [2]Department of Geophysical, Atmospheric and Planetary Sciences, Tel Aviv University, Tel Aviv, Israel, [3]Centrum Wiskunde and Informatica, Amsterdam, Netherlands, [4]Department of Life and Natural Sciences, Open University of Israel, Ra'anana, Israel

Abstract Atmospheric electricity has been detected in all gaseous giants of our solar system and is therefore likely present also in extrasolar planets. Building upon measurements from Saturn and Jupiter, we investigate how the electromagnetic pulse emitted by a lightning stroke affects upper layers of a gaseous giant. This effect is probably significantly stronger than that on Earth. We find that electrically active storms may create a localized but long-lasting layer of enhanced ionization of up to 10^3 cm^{-3} free electrons below the ionosphere, thus extending the ionosphere downward. We also estimate that the electromagnetic pulse transports 10^7 J to 10^{10} J toward the ionosphere. There emissions of light of up to 10^8 J would create a transient luminous event analogous to a terrestrial "elve."

1. Introduction

Giant gaseous planets were the first planets to be observed outside our solar system and, since they are favored by ground-based detection, still comprise a large part of the exoplanets discovered so far. Broadly defined as having 0.3 to 10 Jupiter masses and an atmosphere dominated by H_2, it is presently estimated that about 20% of G- and K-type dwarf stars host at least one of them within 20 AU (Astronomical Units, 1 AU = 1.4960 × m) [*Cumming et al.*, 2008; *Howard*, 2013]. The two giant planets in our solar system (Jupiter and Saturn) have been long studied both from ground-based telescopes and from visiting spacecraft.

One remarkable outcome of such investigation has been the detection of atmospheric electricity in them. Our understanding of convective storms and the direct optical observations from Jupiter and Saturn suggests that in these planets lightning occurs at deep layers of the atmosphere [*Yair et al.*, 2008], precluding any direct observation of its local chemical impact. We know, however, that on Earth the lightning-generated electromagnetic fields couple lower and upper layers of the atmosphere. This coupling is sometimes directly visible in the mesosphere or lower ionosphere as a transient luminous event (TLE) such as a sprite, halo, or elve—we review these phenomena below. Besides this visible manifestation, electric storms have additional detectable effects on the lower ionosphere, including long-lasting changes in the atmospheric conductivity [*Haldoupis et al.*, 2013; *Shao et al.*, 2013; *Gordillo-Vázquez and Luque*, 2010]. It is therefore natural to wonder about the existence and relevance of such electromagnetic coupling in the atmospheres of gaseous giants.

Previous work by *Yair et al.* [2009] and *Dubrovin et al.* [2010] focused on the impact of the quasi-static electric field created by charges in a thundercloud—this is the mechanism that, on Earth, drives sprites and halos. This was later extended by *Dubrovin et al.* [2014] to include also the induction field, which turns out to be dominant in giant planets in the region directly above the originating discharge. Here we consider the full radiated field including the electromagnetic pulse, which is responsible for elves on our planet. As we will argue below, the best available characterization of lightning in gaseous giants suggests that an electromagnetic pulse influences the upper atmosphere much more strongly on the gaseous giants than on Earth.

In this work we focus on Jupiter and Saturn, the two planets with the most abundant lightning observations. In each of them we investigate the atmospheric propagation and the local impact of a lightning-generated electromagnetic pulse. Our results indicate that, in some cases, a lightning discharge in the deep atmosphere induces an extended layer of enhanced ionization below the ionosphere. Given that H_2 and He are

weakly attaching gases, an ionization enhancement may persist for several seconds and alter the surrounding chemical composition. We also estimate the intensity of light emitted from extraterrestrial elves; this may guide attempts to detect them or, alternatively, constrain the physics of extraterrestrial lightning from the absence of elve observations.

The paper is organized as follows. In section 2, we review the electromagnetic coupling between terrestrial atmospheric layers; then we turn to giant planets in our solar system and discuss existing observations of lightning and previous investigations on the possibility of sprites and halos. With this information, we use a simple scaling argument to motivate the study of electromagnetic pulses radiated from an impulsive discharge. Section 3 describes an electromagnetic finite difference time domain (FDTD) code that incorporates impact ionization and dielectric relaxation of the atmosphere. In section 4, we apply this code to the atmospheres of Saturn and Jupiter. We conclude with a brief discussion of our results and their relevance in section 5.

2. Lightning-Induced Troposphere-Ionosphere Coupling

2.1. Terrestrial Transient Luminous Events

In order to understand the possible electromagnetic mechanisms that couple lower and upper atmospheric layers in gaseous giants, let us briefly review the present understanding of such coupling on Earth. In the literature, these coupling mechanisms are often referred to as transient luminous events (TLEs), thus emphasizing their most conspicuous feature: the emission of visible light. However, we should bear in mind that these emissions are not the only manifestation of this coupling: the conductivity of the lower ionosphere is also altered, as evidenced from observations of reflecting very low frequency radio waves [*Inan et al.*, 2010]. The low-altitude electrical activity of a thunderstorm may also induce complex changes in the upper atmospheric chemistry [*Parra-Rojas et al.*, 2013; *Gordillo-Vázquez*, 2008, 2010] or accelerate electrons up to high energies [*Dwyer et al.*, 2012; *Luque*, 2014].

A lightning-induced electromagnetic field acts on the upper atmosphere by accelerating free electrons that may acquire enough energy to cause chemical alterations to the molecules on which they impact. Above certain threshold, the electrons liberate further electrons by impact ionization, thus multiplying the effect of the initial field. For a given gas composition, the energy distribution of electrons is, to a very good approximation, a function only of the ratio between the local electric field E and the neutral particle density n; this ratio E/n is called reduced electric field and is commonly measured in Townsend (1 Td = 10^{-17} V cm^2).

In 1925, *Wilson* [1925] realized that an uncompensated charge left in a thundercloud after a lightning stroke, together with its interaction with the Earth's conducting surface, creates an electric field that decays as a dipolar field $E \sim z^{-3}$, where z is the altitude. On the other hand, due to the exponential decay of atmospheric density n the reduced electric field E/n diverges for z to ∞. Therefore, there exists an altitude where the field is strong enough to accelerate the available electrons sufficiently to affect the neutral molecules.

This effect was spectacularly observed in 1989 by *Franz et al.* [1990] in the form of a sprite: a huge luminous emission spanning altitudes from 50 km to 90 km. This first detection spawned a new research field that has now expanded to investigate many other kinds of TLEs discovered in the last decades. For more details, we refer to *Ebert et al.* [2010] and *Pasko et al.* [2012].

The mechanism sketched by Wilson deals with the quasi-electrostatic field created by a stationary or slowly varying cloud charge. This mechanism is known to induce two types of TLEs: sprites and halos. Sprites, the first observed TLEs, are very luminous filamentary electric discharges composed by streamers; halos are diffuse, pancake-like emissions that occur at about 85 km altitude.

Besides this quasi-electrostatic coupling (QE), the lightning discharge also radiates an electromagnetic pulse (EMP). *Inan et al.* [1991] and, later, *Taranenko et al.* [1993a, 1993b] investigated theoretically the effects of the EMP on the lower ionosphere and predicted significant ionization and emissions of light. As was the case with Wilson's study, observations also bore out this latter prediction, first with recordings from the Space Shuttle by *Boeck et al.* [1992] and then, more clearly, by the measurements of *Fukunishi et al.* [1996], who coined the acronym ELVE (Emissions of Light and Very Low Frequency Perturbations due to Electromagnetic Pulse Sources). Elves are expanding, ring-shaped light emissions located at about 100 km altitude, centered above the originating lightning and lasting less than or about 1 ms.

Kuo et al. [2008] estimated the energy deposition into the upper atmosphere due to sprites, halos, and elves at, respectively, 22, 14, and 19 MJ per event; however, due to the much higher frequency of elves, they are the dominant mechanism of electromagnetic energy transport from lightning into the upper atmosphere, the respective rates being 22, 14, and 665 MJ/min. Note, however, that these estimations are based on counts of detected events; that is, only those luminous enough to be observed. The global energy transported due to dimmer events is harder to estimate. We emphasize here that whereas sprites are essentially nonlinear phenomena and have therefore a lower threshold of intensity below which they are not physically possible, halos and elves do not possess such essential nonlinearity and one can in principle conceive of halos and elves with infinitesimally weak brightness.

2.2. Lightning in Gaseous Giants

We currently possess evidence of lightning in all four gaseous and ice planets of the solar system. The Voyager mission detected radio emissions attributed to lightning in Jupiter [*Gurnett et al.*, 1979], Saturn [*Warwick et al.*, 1981], Uranus [*Zarka and Pedersen*, 1986], and Neptune [*Gurnett et al.*, 1990; *Kaiser et al.*, 1991]. No other mission has since visited Uranus and Neptune, but much more evidence and information were accumulated about lightning in the two giants, Jupiter and Saturn.

Voyager 1 already detected optical emissions from Jupiter lightning [*Cook et al.*, 1979]. Since then, every spacecraft that has approached this giant planet has imaged lightning flashes from its nightside: Galileo [*Little et al.*, 1999], Cassini [*Dyudina et al.*, 2004], and most recently, New Horizons [*Baines et al.*, 2007]. Radio observations, such as the detection of sferics inside the Jovian atmosphere by the Galileo probe [*Rinnert and Lanzerotti*, 1998], complement these optical observations.

The situation is rather similar regarding Saturnian lightning. Although optical images of lightning in Saturn were obtained only recently [*Dyudina et al.*, 2010], these are now complemented by observations even on the dayside of the planet [*Dyudina et al.*, 2013]. Besides, the still-operating Cassini spacecraft [*Fischer et al.*, 2008] has recorded thousands of radio pulses termed *Saturn electrostatic discharges* (SED) emitted from electric storms. *Zakharenko et al.* [2012] used coincidence analysis with SED recordings to indicate detection of Saturnian lightning from the Earth-based large radio telescope UTR-2.

The evidence presently at hand leads to a few conclusions. First, lightning is probably prevalent in all cold gaseous giant planets, with the required charge separation likely occurring in the deep water-ice layers [*Borucki and Williams*, 1986; *Dyudina et al.*, 2002, 2010]. Second, the estimated energy released by both Saturnian and Jovian lightning is around 10^{12} J per event [*Borucki and McKay*, 1987; *Yair et al.*, 1995; *Dyudina et al.*, 2010, 2013]. This is roughly 10^3 times larger than the energy typically released by terrestrial intracloud lightning. Finally, although the characteristic duration of a lightning stroke in Saturn or Jupiter is uncertain, the high-frequency spectrum of SED recordings, combined with the above estimate of released energy, suggests a duration similar to that of terrestrial lightning from some tens of microseconds up to about 1 ms [*Fischer et al.*, 2006; G. Fischer, private communication, 2013].

Here we must mention that, while it is reasonable to extend these conclusions to all or most cold gas giants, including those outside our solar system, they are probably not valid for so-called "hot Jupiters," where water exists only in its vapor phase [*Aplin*, 2013]. However, lightning-like discharges may still exist in those planets if, as proposed by *Helling et al.* [2011], dust particles replace ice and graupel in the process of charge separation.

For more details about extraterrestrial lightning, we refer to the recent reviews by *Yair et al.* [2008] and *Yair* [2012].

2.3. TLEs in Other Planets

The discovery of troposphere-mesosphere electromagnetic coupling on Earth led some researchers to investigate the possibility of similar mechanisms in other planets. *Yair et al.* [2009] first discussed the existence of sprites in other bodies of the solar system, merging Wilson's classical estimate (as discussed above) with present knowledge about electrical phenomena in these planets. *Dubrovin et al.* [2010] investigated the possible optical emissions of these sprites with laboratory models. Recently, *Dubrovin et al.* [2014] focused on Saturn and included not only the quasi-static field but also the induction field and the effects of dielectric relaxation. However, its zero-dimensional approach limited this model to the region directly above the lightning discharge. Because the EMP vanishes on the vertical axis of the discharge dipole, it cannot be modeled with that approach. But, as we mentioned above, on Earth the EMP dominates the energy

transport from lightning toward the ionosphere. Furthermore, as we shall see now, the reduced electric fields created by the electromagnetic pulse in gaseous giants are likely significantly higher than on Earth, so they may have a stronger chemical impact on the upper atmosphere.

2.4. Scaling of Reduced Electric Fields

Since high electric fields lead to breakdown, the effect on the upper atmosphere of a lightning flash can be strongly nonlinear and it is therefore difficult to estimate. However, it is useful to momentarily neglect breakdown and dielectric relaxation and perform a preliminary analysis of the peak-reduced fields, extending the discussion that we initiated in *Dubrovin et al.* [2014]. This serves us only to motivate the study of EMP fields; below we consider realistic models that include relaxation and breakdown.

Assume that an intracloud lightning stroke transports vertically a charge Q for a distance h within a time scale τ. This can be approximated by a time-dependent electric dipole $P=Qh$ oriented along the z axis. For cloud-to-ground discharges the *charge moment change* (M) is commonly defined as the product of the amount of charge and the height from which it was lowered to the ground. In that case the dipole is formed by a charge in the cloud and its mirror image below the Earth's conducting surface, separated by twice the cloud's altitude so that $P=2M$. To be consistent with the existing literature we will use the charge moment change $M=P/2$ to quantify the dipolar moment both of cloud-to-ground and intracloud discharges.

Here and below we model the lightning discharge with a vertical channel. We do not know the precise discharge geometry of extraterrestrial lightning but, by analogy with thunderclouds on Earth, where gravity plays a major role in cloud electrification, it is reasonable to assume that in other planets the charges inside a cloud are also vertically separated. Most terrestrial intracloud discharges connect two levels of opposite polarity [*Shao and Krehbiel*, 1996], involving a net vertical charge transfer. In Jupiter and Saturn, shear winds may be stronger, drifting the charged layers apart and leading to discharges with a large horizontal component. However, since these mechanisms are quite uncertain, we believe that presently the most reasonable approximation is to assume a mostly vertical charge transport in all planets.

The electromagnetic field created by a radiating dipole can be divided in three parts [*Jackson*, 1975]: a quasi-static field, an induction field, and a radiation field, each of them decaying as, respectively, $1/r^3$, $1/r^2$, and $1/r$. It is illustrative to estimate these components for Earth, Jupiter, and Saturn.

The quasi-static electric field is determined exclusively by the magnitude of the electric dipole. On the axis of the dipole the quasi-static electric field reads

$$E_{\mathrm{QE}} = \frac{M}{\pi\epsilon_0(z-z_P)^3}, \tag{1}$$

where ϵ_0 is the electric permittivity of vacuum. The altitudes z and z_P correspond, respectively, to where the electric field is measured and to where the dipole is located.

The induction field is proportional to the discharging current, $\mathrm{d}Q/\mathrm{d}t$. We obtain an analytic order-of-magnitude approximation to this field from the peak field radiated by a harmonic dipole antenna of frequency $\omega = 1/\tau$:

$$E_{\mathrm{ind}} \approx \frac{M}{\pi\epsilon_0 c\tau(z-z_P)^2}, \tag{2}$$

where c is the speed of light.

Finally, the radiation field is proportional to the time derivative of the discharging current, $\mathrm{d}^2Q/\mathrm{d}t^2$:

$$E_{\mathrm{rad}} \approx \frac{M\sin\alpha}{2\pi\epsilon_0 c^2\tau^2 r} = \frac{M\sin 2\alpha}{4\pi\epsilon_0 c^2\tau^2(z-z_P)}, \tag{3}$$

where c is the speed of light, α is the angle between the vertical and the propagation path, and $r = (z-z_P)/\cos\alpha$ is the distance from the emitting dipole.

The ratio between the fields in equations (1)–(3) scales as $E_{\mathrm{QE}} : E_{\mathrm{ind}} : E_{\mathrm{rad}} \sim 1 : (z/c\tau) : (z/c\tau)^2$. Hence, if the discharge times are similar in different planets, as they apparently are, the radiation field dominates relative to the QE field in planets with long typical distances.

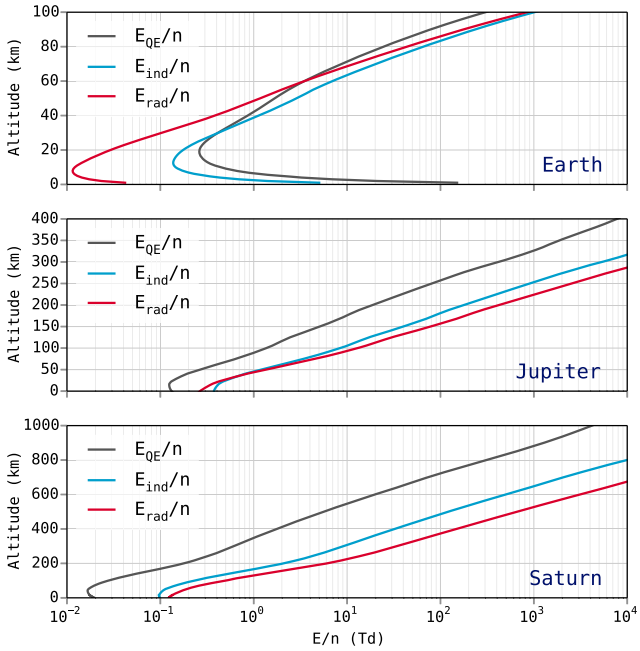

Figure 1. Approximate scaling of the quasi-static, the induction, and the radiation-reduced electric fields on Earth, Jupiter, and Saturn. We used typical charge moment changes M and lightning discharge times τ. We plotted the fields in (1)–(3), which do not account for dielectric relaxation or breakdown of the atmosphere; the plots here are intended solely to illustrate the different scalings of E_{QE}, E_{ind}, and E_{rad}, which lead to relatively much more intense effects of the radiation field in the gas giants. The charge moment change is $M = 10^2$ C km for Earth and $M = 10^5$ C km for Saturn and Jupiter, whereas the characteristic discharge time is τ=100 μs for the three planets.

We need now to estimate the charge moment change M in Saturn and Jupiter. *Dubrovin et al.* [2014] showed that the energy U_P dissipated by a lightning stroke can be approximated by the electrostatic energy stored by two oppositely charged spheres of radius R and separated a distance h:

$$U_P = \frac{2Q^2}{4\pi\epsilon_0}\left(\frac{3}{5R} - \frac{1}{2h}\right). \quad (4)$$

As we mentioned above, the energy released by a lightning stroke in a gaseous giant is estimated as $\sim 10^{12}$ J or about 10^3 times the median terrestrial value [*Dyudina et al.*, 2010]. Depending on assumptions about h and R, the charge moment change, M, of a discharge in Saturn and Jupiter can be between 10^4 C km and 10^6 C km, which is about 10^2–10^4 times larger than on Earth.

We can now illustrate the scaling behavior of electric fields in Figure 1, where we plotted E_{QE}, E_{ind}, and E_{rad} using $M = 10^2$ C km for Earth and $M = 10^5$ C km for Saturn and Jupiter and $\tau = 100$ μs for the three planets; as we saw above, this time is valid at least for Earth and Saturn, and we extrapolate it also for Jupiter. The dipole representing the discharge is located at $z_P = 0$ on Earth, $z_P = -150$ km on Saturn, and $z_P = -85$ km on Jupiter (relative to the 1 bar level in the latter cases where 1 bar = 10^5 Pa). The radiation field acts at points where the propagation angle is significantly higher than zero (i.e., at points away from the vertical axis defined by the lightning); wherever this condition is fulfilled the geometric factor $\sin 2\alpha$ does not have a strong effect on the order of magnitude of E_{rad}, so for our plot we assumed $\sin 2\alpha \approx 1$. The gas density for Earth is obtained from the U.S. Standard Atmosphere [*United States Committee on Extension to the Standard Atmosphere*, 1976]; the densities for Jupiter and Saturn are as explained below. The altitudes extend roughly up to the lower edge of the ionosphere; the electric field is quickly screened at higher altitudes and therefore unlikely to have a significant effect.

The plots show that, whereas the three components of the reduced field are roughly comparable on Earth, in the gas giants the radiation field is much stronger than the static and induction components. The reduced field E_{rad}/n reaches 100 Td at about 150 km in Jupiter and 400 km in Saturn; reduced electric fields of this magnitude are likely to impact significantly on the chemistry of the atmosphere at these altitudes.

We must emphasize, however, that the fields in Figure 1 must not be taken at face value but rather as an illustration of the scaling; the actual electric fields are lower once we account for dielectric relaxation.

3. FDTD Code

A correct assessment of the propagation of an electromagnetic pulse and its interaction with the upper layers of an atmosphere requires solving the Maxwell equations and including nonlinear effects whereby the atmospheric conductivity is affected by the local fields. For this purpose we developed a finite difference time domain (FDTD) code.

For an introduction to FDTD modeling of electromagnetic wave propagation, we refer to the textbook by *Inan and Marshall* [2011]. FDTD codes have successfully modeled the lightning-ionosphere interactions

on Earth [*Taranenko et al.*, 1993b; *Veronis et al.*, 1999; *Cho and Rycroft*, 2001; *Rowland et al.*, 1996; *Marshall et al.*, 2010; *Marshall*, 2012]. Here we used the GREMPY code (GRanada ElectroMagnetic PYthon simulator): source code and documentation are available from https://github.com/aluque/grempy.

Our code is partly based on the algorithm described by *Marshall* [2012], but here we implement a Cartesian 2-D grid that assumes cylindrical symmetry around the vertical axis defined by the lightning and neglects the curvature of the modeled planet. In this model we couple Maxwell's equations to two other equations: one to calculate the electric current density from the local electric field and one to update the electron density due to impact ionization.

We solve Maxwell's equations for the electric and magnetic fields, **E** and **H** using the leapfrog centered differences scheme of *Yee* [1966]. Ideally, the outer boundaries of the simulation domain should completely absorb all radiation; we approximated these ideal boundary conditions using convolutional perfectly matched layers [*Inan and Marshall*, 2011] with a thickness of 10 simulation cells.

To calculate the current density **J**, we use the approximation that it is dominated by the light and very mobile electrons (the mobility of ions is about 100 times smaller than the electron mobility), and we obtain **J** self-consistently by solving Langevin's equation,

$$\frac{\partial \mathbf{J}}{\partial t} + \nu \mathbf{J} = \omega_p^2 \epsilon_0 \mathbf{E}, \tag{5}$$

where ν is the effective collision frequency between electrons and the background gas, $\nu = e/\mu m_e$ (μ: electron mobility, e: elementary charge, m_e: electron mass). The electron mobility depends on the local reduced electric field E/n, but it can be approximated as constant in the range 10 Td to 10^3 Td, which covers the most significant effects of the electric field. We used $\mu = (1.2 \times 10^{22}\ \mathrm{cm^{-1}\ V^{-1}\ s^{-1}})/n$. The plasma frequency of electrons ω_p is defined as

$$\omega_p = \left(\frac{e^2 n_e}{m_e \epsilon_0} \right)^{1/2}, \tag{6}$$

where n_e is the density of free electrons. We solve equation (5) simultaneously to the Maxwell equations using the procedure of *Lee and Kalluri* [1999].

Langevin's equation (5) can be derived by calculating the time derivative of $\mathbf{J} = -en_e\mathbf{v}_d$, where $\mathbf{v}_d$ is the electron drift velocity. The electron acceleration $\mathrm{d}\mathbf{v}_d/\mathrm{d}t$ is set by an electrostatic force $\mathbf{F}_E = -e\mathbf{E}$ and a friction force $\mathbf{F}_F = -m_e\nu\mathbf{v}_d$. In the derivative of $en_e\mathbf{v}_d$, we also find a term $e\mathbf{v}_d\partial_t n_e = \nu_i\mathbf{J}$, where ν_i is the effective ionization rate (see below). We have neglected this term since $\nu_i \ll \nu$. Note also that the limit of (5) for long times is Ohm's equation $\mathbf{J} = \sigma\mathbf{E}$ with conductivity $\sigma = \omega_p^2\epsilon_0/\nu = e\mu n_e$. As we will describe below, the electron density n_e is updated self-consistently with the electric field, introducing a significant nonlinearity in the model.

In (5) we neglect the effect of a background magnetic field $\mathbf{B_0}$. The validity of this approximation is determined by the comparison between the electron gyrofrequency $\nu_G = eB_0/2\pi m_e$ and the momentum transfer frequency ν. The ratio between these two magnitudes, $\alpha = \nu_G/\nu$, provides a dimensionless measure of the relevance of the magnetic field. Since the momentum transfer frequency ν is proportional to the gas density n, we can write $\nu = e/m_e\mu = en/m_e\kappa$, where $\kappa = \mu n$ is called *reduced mobility* and does not depend on the gas density. Then α equals unity for a value n_B of the gas density satisfying

$$n_B = \frac{\kappa B_0}{2\pi}. \tag{7}$$

The background magnetic field $\mathbf{B_0}$ becomes relevant for densities below n_B. In Table 1, we show the approximate values of the magnetic field on Earth, Saturn, and Jupiter together with the resulting n_B and the altitude where that density is reached. Note that these estimations assume that the mobility does not depend on the electric or magnetic fields and has the value given above.

Most of our modeling applies to gas densities significantly higher than n_B, but at the highest altitudes in consideration, we cannot overlook the possibility that the direction and magnitude of $\mathbf{B_0}$ has some impact on the lightning-ionosphere interaction. However, investigating this issue would require a 3-D FDTD code and this falls outside our present computational capability.

Table 1. Conditions Where the Background Magnetic Field Can Be Neglected[a]

Planet	B_0 (μT)	κ (cm^{-1} V s^{-1})	n_B (cm^{-3})	h_B (km above 1 bar)
Earth	40	1×10^{22}	6.3×10^{12}	100
Saturn	20	1.2×10^{22}	3.8×10^{12}	870
Jupiter	200	1.2×10^{22}	3.8×10^{13}	330

[a]For each planet we list a typical value for the background magnetic field (B_0) at the equator, the average reduced mobility κ, the minimal gas density (n_B) for which the magnetic field can be neglected, and the altitude (h_B) where n_B is reached.

Besides the self-consistent electric current modeled by (5) the sources in the Maxwell equations also contain the current of the causative lightning, which we model as an independent, prescribed $\mathbf{J}_L$. We consider this term as a vertical current located in the axis of symmetry and spanning altitudes between two predefined values z_0 and z_1. The time dependence of the current is biexponential,

$$I(t) = \frac{Q}{\tau_1 - \tau_2}\left(e^{-t/\tau_1} - e^{-t/\tau_2}\right), \tag{8}$$

where τ_1 and τ_2 are, respectively, the total and the rise time of the lightning stroke and Q is the total charge transferred by the stroke. The charge moment change of this discharge is $M = Q(z_1 - z_0)/2$.

The density of free electrons is updated self-consistently as

$$\frac{\partial n_e}{\partial t} = n_e \nu_i(E/n), \tag{9}$$

where ν_i is the effective ionization rate of the medium. We solve equation (9) implicitly by updating n_e at each time step as $n_e^{t+\Delta t} = n_e^t(1 - \nu_i(E^t/n)\Delta t)^{-1}$.

We obtain the dependence of ν_i on the reduced electric field using the Boltzmann equation solver BOLSIG+ developed by *Hagelaar and Pitchford* [2005]. For a given atmospheric composition, ν_i is calculated as

$$\nu_i(E/n) = n \sum_s x_s k_s(E/n), \tag{10}$$

where x_s is the volume fraction of species s, and k_s is the rate coefficient for the impact ionization of s. The cross sections were obtained from the SIGLO database; they originate from the compilation of cross sections by A. V. Phelps (ftp://jila.colorado.edu/collision_data/) [*Buckman and Phelps*, 1985]. See *Dubrovin et al.* [2014] for a plot of the ionization rates in an atmosphere of H_2:He with a 90:10 volume mixing ratio.

Electron impact cross section for high electron energies are not measured accurately so ν_i is not very reliable for high reduced electric field. For fields above 10^3 Td, we extrapolated ν_i by fitting to a Townsend expression $\nu_i(E/n) = a \times (E/n)\ \exp\ (-bn/E)$ with $a \approx n \times (2.48 \times 10^{-11}$ cm^3 s^{-1} Td^{-1}), $b \approx 2.2 \times 10^{-3}$ Td^{-1}, but with slightly different values for the compositions of Saturn and Jupiter. We do not include attachment, detachment, or recombination processes since, as discussed by *Dubrovin et al.* [2014], they are negligible in H_2:He atmospheres at the time scales of interest.

Note that (9) neglects the transport of electrons due to their drift in the electric field. This is justified by the large length scales and short characteristic times of our system. Even in a reduced electric field $E/n \approx\ 10^3$ Td, electrons drift at a speed of about 10^6 m/s. On the other hand, the traveling EMP acts for less than 1 ms at a given point. In that time a typical electron travels a distance of less than 1 km; this compares with typical distances of hundreds of kilometers. Nevertheless, for longer times the neglected transport terms may play a significant role, particularly if the standing, electrostatic field is strong enough to ignite streamer discharges with much shorter typical distances. This issue, however, falls outside the focus of this paper.

In order to evaluate the emissions of light induced by the EMP in the upper atmosphere, we account for the collisional excitation of molecular hydrogen to the electronic states $H_2\ (d^3\Pi_u)$ and $H_2\ \left(a^3\Sigma_g^+\right)$. We assumed that at the altitudes of interest, the collisional deactivation (quenching) of these states is negligible

[*Bretagne et al.*, 1981] so every excitation of $H_2\left(a^3\Sigma_g^+\right)$ leads to the emission of a photon in a continuum of ultraviolet (UV) wavelengths via the transition

$$H_2\left(a^3\Sigma_g^+\right) \rightarrow H_2\left(b^3\Sigma_u\right) + \gamma_{\text{cont}}. \tag{11}$$

The state $H_2\left(d^3\Pi_u\right)$ decays into $H_2\left(a^3\Sigma_g^+\right)$, so each time it is excited it leads to the emission of two photons, first one in the Fulcher band via

$$H_2\left(d^3\Pi_u\right) \rightarrow H_2\left(a^3\Sigma_g^+\right) + \gamma_{\text{Fulcher}}, \tag{12}$$

and then one in the UV continuum via (11). In our previous work, we showed that these are the dominant processes of light emission excited by electric fields in the upper atmosphere of a planet composed by hydrogen and helium [*Dubrovin et al.*, 2014]. The lifetimes of the two excited states are some tens of nanoseconds [*Astashkevich and Lavrov*, 2002], much shorter than the typical time scales of the EMP pulse, so we consider that light emission proceeds instantaneously after the excitation.

We also evaluate the impact of the EMP on the upper atmosphere by measuring the density of energy that it deposits. This density, u, can be obtained by integrating the work per unit time and volume performed by the electromagnetic field:

$$\frac{\partial u}{\partial t} = \mathbf{J} \cdot \mathbf{E}. \tag{13}$$

This equation is integrated simultaneously with the Maxwell equations, Langevin's equation (5), and the electron density equation (9); however, u does not play any further role and is used only as a diagnostic output. Part of this deposited energy increases the temperature of the gas while other fractions excite rotational, vibrational, and electronic levels. Ultimately the energy will be either thermalized or radiated away, but here we will not investigate the paths that lead to that result.

4. Results

4.1. Saturn

We will first study the effects of a lightning EMP in Saturn. As discussed by *Dubrovin et al.* [2014], the electron density in the Saturnian atmosphere below the 1000 km level is uncertain. *Moore et al.* [2004] present an electron density profile with a density $n_e \approx 10^2$ cm^{-3} at about 1000 km and a sharp decay downward. In contrast, *Moses et al.* [2000] and *Galand et al.* [2009] assume the photoionization of a carbo-hydrate layer between 600 km and 1000 km, predicting a relatively uniform density of free electrons $n_e \approx 10^2$ cm^{-2} within this layer. These two theoretical profiles, which we respectively name (A) and (B,) are plotted in Figure 2 where we also show the density of the background gas, obtained by *Festou and Atreya* [1982]. In our simulations we used a 90:10 volume mixture ratio of H_2:He (this corresponds to a mass ratio of 82:18).

The lightning stroke in Saturn is modeled after *Dubrovin et al.* [2014], with the biexponential time profile (8) and total and rise times $\tau_1 = 1$ ms, τ_2=100 μs. The stroke current is assumed to be located between $z_0 = -160$ km and $z_1 = -130$ km.

The FDTD simulation domain consists in a cylindrical box with a radius of 3000 km spanning altitudes from −1000 km to 1250 km. We used a spatial resolution $\Delta r = \Delta z = 1$ km and time steps Δt=200 ns. The total running time of the simulations was about 2 days in a standard desktop computer.

We analyze here four simulations, with charge moment changes $M = 10^4$ C km and $M = 10^5$ C , km and the two possible electron density profiles, with and without a carbo-hydrate (CH_x) layer. Figure 3 shows three snapshots of the reduced electric fields from these simulations.

Whereas in the presence of a CH_x layer the reduced electric field peaks at about 150 Td, if that layer is absent, E/n reaches extremely high values above 10^3 Td. Those extreme values quickly ionize the atmosphere, leading to a fast relaxation, as shown, e.g., in the region of decreased E/n at $t = 3$ ms. The dynamics in those cases becomes highly nonlinear and complex, as exemplified in the intricate structures seen at $t = 4$ ms.

The effects of these electric fields on the upper atmospheric layers are summarized in Figure 4, where we plot the electron density, the number of emitted photons per unit volume, and the density of deposited

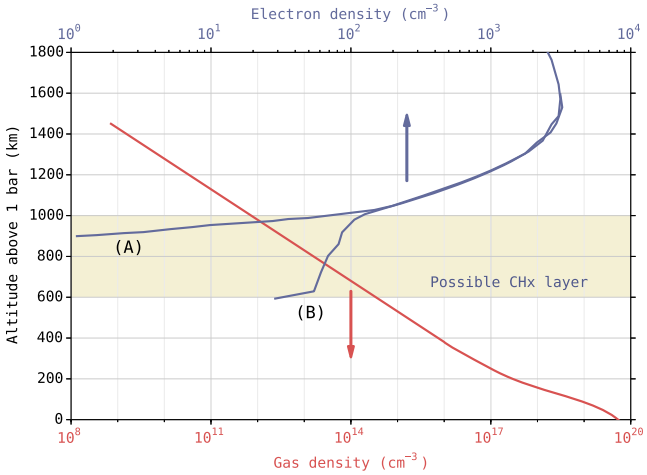

Figure 2. Density profiles of the background gas and initial free electrons in Saturn used in our simulations. The gas density was obtained by *Festou and Atreya* [1982] by interpolating two measured data sets. We analyze two possible profiles for the electron density: (A) with a high ionosphere at 1000 km and (B) with the ionosphere extending down to 600 km due to the presence of a hydrocarbon (CH_x) layer.

energy left by the EMP, all evaluated after a long time (20 ms). We also provide plots of the net increase in electron density in the supporting information.

The electron density is barely affected by lightning strokes with charge moment change $M = 10^4$ C km, either in the presence or the absence of a CH_x layer. However, the EMP produced by a charge moment change $M = 10^5$ C km leaves behind a layer of significantly enhanced electron density. In our profile (A), the electron density acquires a peak at 700 km with a value of 10^3 cm^{-3}; in profile (B), the peak is located around 600 km with a value of a few times 10^2 cm^{-3}.

Dubrovin et al. [2014] estimate the rate of attachment for low fields as $k_{att} \approx 2 \times 10^{-15}$ cm^3 s^{-1}. According to the gas densities of Figure 2, the electron lifetimes $\tau = 1/[H_2]k_{att}$ around the peaks are about 6 s and 3 s for profiles (A) and (B), respectively. These long lifetimes suggest that above a thunderstorm with more than about one flash per second, there may exist a long-lived layer of enhanced electron density in the upper atmosphere.

The possibility of optically detecting elves in Saturn is determined by their total photon emissions, which we estimate in Figure 4 (middle column). Assuming that the wavelength of these photons is close to

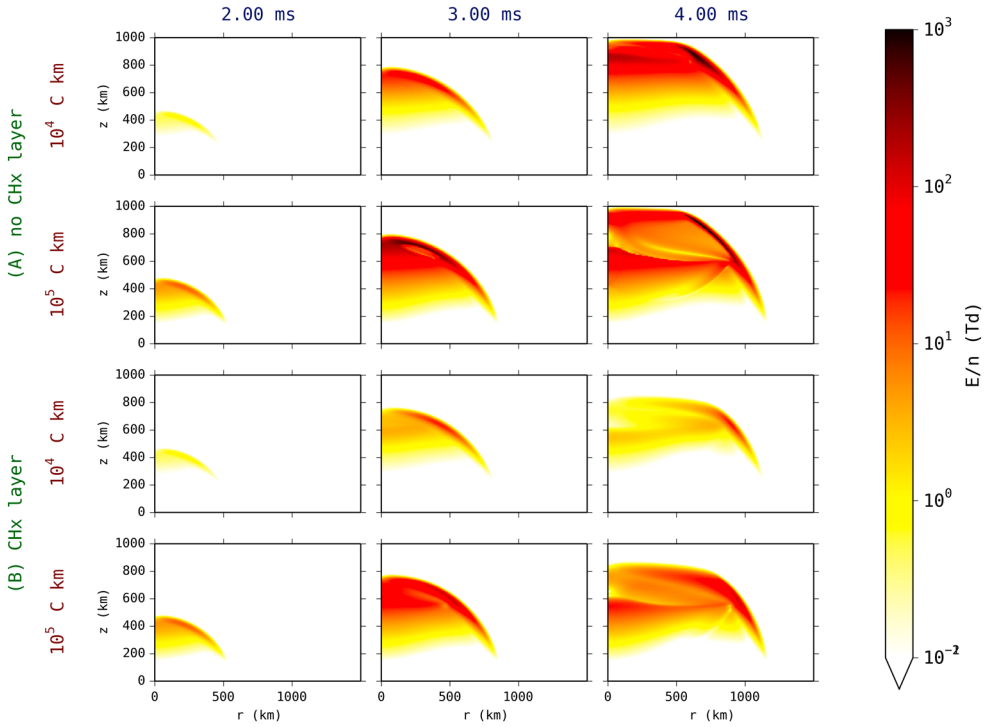

Figure 3. Reduced electric field E/n created in the atmosphere of Saturn due to a lightning stroke. We test two possible values for the charge moment change of the stroke, $M = 10^4$ C km and $M = 10^5$ C km, and the two possible profiles of the electron density plotted in Figure 2. For each of the four resulting simulations, we show three snapshots of the reduced electric field.

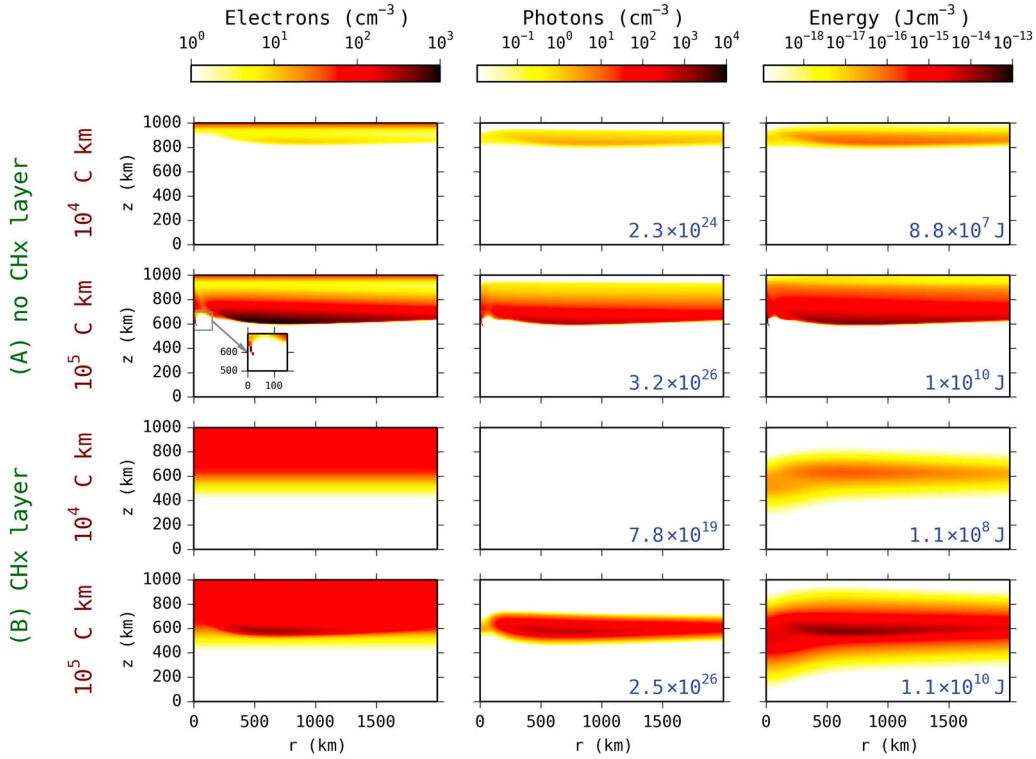

Figure 4. Effects of a lightning stroke on the Saturnian upper atmosphere as reflected in the (left column) electron density, (middle column) photon emissions, and (right column) deposited energy density. The number in the lower right corner of the panels in the middle and right columns expresses, respectively, the total number of emitted photons and the total energy deposited in the upper atmosphere. In the supporting information we provide plots of the net increase in electron density. All the panels reflect the situation 20 ms after the stroke. The inset in the electron density for $M = 10^5$ C km zooms into the small filamentary feature that we have called *pseudostreamer* and is discussed in the text.

$\lambda = 300$ nm, we obtain the total optical energies from Saturnian elves as $E_{opt} = Nhc/\lambda$, where N is the number of emitted photons and h is Planck's constant. For a charge moment change of $M = 10^5$ C km, for both electron density profiles, these energies are slightly above 10^8 J, which is comparable to the optical energy emitted by the lightning itself that *Dyudina et al.* [2013] estimate as 10^9 J.

This raises the possibility that elves can be imaged from spacecraft orbiting Saturn, such as Cassini and its ISS instrument [*Porco et al.*, 2004]. To exemplify how an elve would appear from the vantage point of an orbiting spacecraft, looking at the nadir we integrated in the vertical direction the photon density plotted in Figure 4. We selected the case $M = 10^5$ C km, with profile (B). The result, shown in Figure 5, exhibits the characteristic torus-like shape familiar from terrestrial elves. The radius of the peak emissions in the torus can be estimated from our simplified expression for the radiation field (3). There we see that for fixed z the electric field peaks when $\alpha = \pi/2$, i.e., at a distance $\rho = (z - z_p)$ from the axis. In our simulations $z_p = -145$ km and the elve appears around the lower edge of the ionosphere at $z \approx 600$ km, which gives $\rho = 745$ km, which is approximately consistent with the peak emissions in Figure 5.

Returning to Figure 4, the right column plots the energy deposited by the EMP into the upper atmosphere. For the parameters that we considered in our simulations, the total energy transferred from the lightning discharge toward upper layers ranges from about 10^7 J to 10^{10} J. Taking an estimate of about 10 flashes per second in the large 2011 storm [*Dyudina et al.*, 2013], we obtain a total power transferred by EMPs of about 10^8 W to 10^{11} W. *Dyudina et al.* [2013] estimates the storm's convective energy flux at 10^{17} W, a value similar to the better constrained total radiative cooling rate 2×10^{17} W that we can obtain from the emitted power ~ 5 W/m^2 measured by *Li et al.* [2010]. These values imply that although the energy transport in EMPs may have relevant local effects, it is too low to influence the cooling of the Saturnian atmosphere.

For the highest charge moment, $M = 10^5$ C km, and profile (A) a small filamentary feature is found close to the axis. This feature, that we may call *pseudostreamer*, develops from the screening ionization wave created

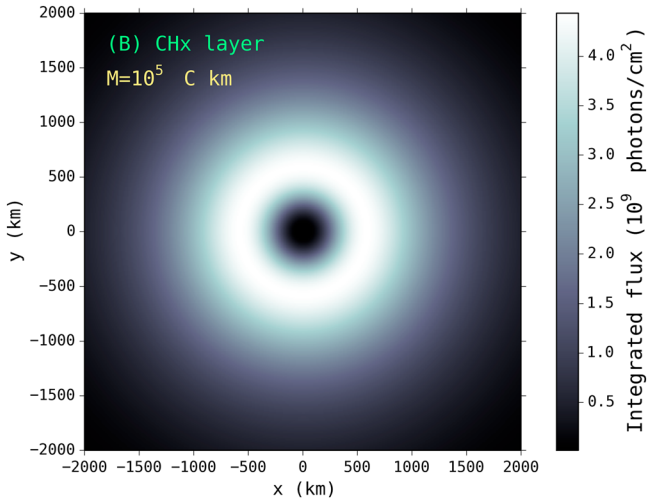

Figure 5. Mock-up of an image of an elve in Saturn as seen at the nadir from an orbiting spacecraft. We show here the column-integrated photon emissions shown in Figure 4 for the case $M = 10^5$ C km, profile (B).

by the quasi-electrostatic field by a mechanism similar to that described by *Luque and Ebert* [2009]. However, the simulations here do not include the full transport of electrons and they do not have enough resolution and are therefore inadequate for streamer modeling [*Luque et al.*, 2008; *Luque and Ebert*, 2012]. Therefore, we consider this feature as an artifact, although it points to a likely inception of a sprite. Note that the presence of this pseudostreamer does not influence the interaction between the ionosphere and the EMP, which is the main focus of this paper.

4.1.1. Comparison With a Planar Approximation

In a previous work [*Dubrovin et al.*, 2014], we used a planar approximation to estimate the effect of an electric field in the upper atmosphere of Saturn in the axis directly above a dipolar discharge. In that approach the electric field evolves as

$$\frac{\partial E}{\partial t} = \frac{\partial E_p}{\partial t} - \frac{\sigma E}{\epsilon_0}, \tag{14}$$

where σ is the local conductivity and E_p is the field that would be created by the dipole in the absence of atmospheric screening or reflection (note that screening is created by the second term in the right-hand side of (14), whereas reflection is not included at all in the planar approximation). The field E_p contains the quasi-electrostatic and the induction components discussed in section 2.4; the radiation field vanishes at the axis of the dipole and hence does not play any role directly above the discharge.

We can now use the FDTD code to investigate the validity of the planar approximation (14). Figure 6 shows the vertical component of the reduced electric field calculated by (14) and by the FDTD code at the axis $r=0$ at three altitudes. We analyze here the case with $M=10^5$ C km with profile (B). At the lowest altitude, 400 km, the planar approximation is very accurate and the only significant difference between the two results is the effect of a reflected wave around 3.5 ms.

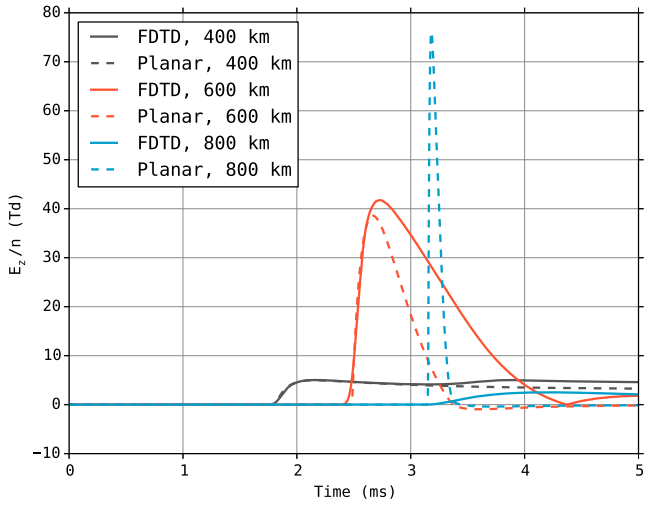

Figure 6. Reduced electric fields created by a discharge with charge moment change $M = 10^5$ C km with the ionospheric profile (B) (i.e., Figure 3, second row). We compare the estimations of the FDTD code (solid lines) with the planar approximation (14) (dashed). The planar approximation is remarkably accurate below the ionosphere but breaks down at high altitudes.

Somewhat above, at 600 km, the planar approximation still provides a reasonable estimation of the peak field but it underestimates the relaxation time. The reason is that in the planar approximation we overestimate the screening field when we assume that a current on the axis extends indefinitely in the transverse direction and creates an infinite plane of charge. In reality the current decreases away from the axis and does not screen the field so efficiently.

Finally, the outcomes of the two codes are very different above the

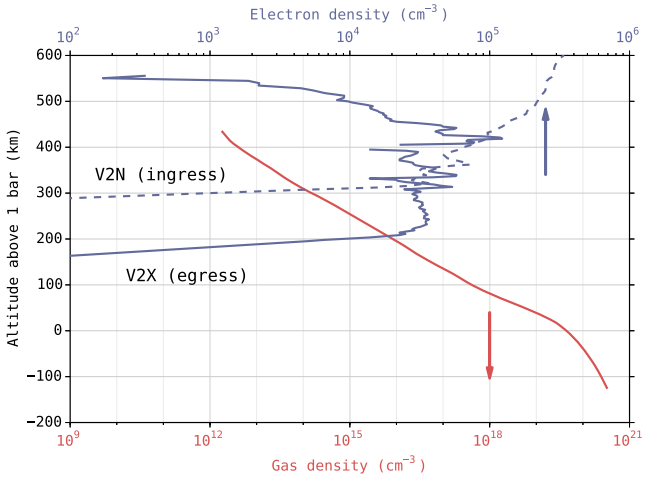

Figure 7. Density profiles of the background gas and initial free electrons in Jupiter used in our simulations. The gas density was obtained by imposing hydrostatic equilibrium to the pressure-temperature relationship obtained by the Galileo probe. The electron density profiles are from Voyager 2 radio occultations. The V2N profile was obtained at ingress (local dusk), whereas V2X was measured at egress (local dawn). Note, however, that it is unclear how strongly the profiles depend on the local time.

ionosphere. Whereas in the FDTD code the field is almost completely reflected and does not reach 800 km, the planar approach predicts a sharp peak that is quickly screened. Here the limitations of (14) are in full sight: a zero-dimensional model does not account for the reflection of a propagating wave occurring between the source and the point of interest.

The comparison between the two codes therefore shows that the planar approximation is accurate at the dipole axis but only up to the lower edge of the ionosphere. As *Dubrovin et al.* [2014] predicted that the major effect of the electric field at the axis occurs below the ionosphere, the FDTD introduces only relatively small corrections. However, as we have seen, the lightning-generated electromagnetic field has its most substantive impact away from the axis, not included in this comparison.

4.2. Jupiter

Let us now turn to analyze the propagation of an EMP in Jupiter. The density of free electrons in the Jovian ionosphere was measured by radio occultation by the Voyager [*Eshleman et al.*, 1979; *Hinson et al.*, 1998] and Galileo missions [*Hinson et al.*, 1997]. As discussed, e.g., by *Yelle and Miller* [2007], the obtained electron density profiles fall into two categories: in some cases the density peaks at a high altitude around 1500 km and stays roughly constant in the range 500 km–1000 km; in other cases the peak is located at low altitude, around 800 km with a sharply decaying density below. The reason behind these two different profiles is presently unclear: they are apparently not correlated with latitude or local time.

Here we will use two profiles from the Voyager 2 radio occultation measurements presented by *Hinson et al.* [1998]: the V2N profile has a low-altitude peak and was obtained at ingress, which for Voyager 2 was at dusk, whereas the V2X profile has a high-altitude peak and was measured during the spacecraft egress during local dawn. These profiles are plotted in Figure 7 where we also plot the neutral density obtained from applying the hydrostatic equilibrium equation to the pressure-temperature relationship obtained by the Galileo probe for Jupiter [*Showman*, 2003]. The reaction rates for the Jovian atmosphere are calculated assuming an 89:11 volume mixture ratio of H_2:He (about 80:20 mass ratio).

Lightning in Jupiter is estimated to discharge channels of around 20 km length [*Yair et al.*, 1995], located at pressures of 2 bar to 5 bar [*Desch et al.*, 2002] and releasing an energy of about 10^{12} J [*Desch et al.*, 2002; *Yair et al.*, 2008]. In our model we translated this to a lighting stroke between $z_0 = -95$ km and $z_1 = -75$ km with the same characteristic times that we assumed in Saturn, $\tau_1 = 1$ ms, τ_2=100 μs and charge moment changes $M = 10^4$ C km or $M = 10^5$ C km.

For Jupiter, the FDTD simulation domain consists in a cylindrical box with a radius of 3000 km spanning altitudes from −800 km to 400 km. We used a spatial resolution $\Delta r = \Delta z = 2$ km. Due to the high conductivity resulting from the electron density that we used, Maxwell relaxation occurs extremely fast at high altitudes. Since we use an explicit update for the electromagnetic fields and the electric currents, we had to use very short time steps to avoid numerical instabilities. We used $\Delta t = 10$ ns for a total running time of about 3 weeks with a standard desktop computer.

We show the reduced electric field resulting from the simulations in Figure 8. As in Saturn, the maximum reduced electric field is strongly influenced by the altitude of the ionosphere. For the V2N profile, where

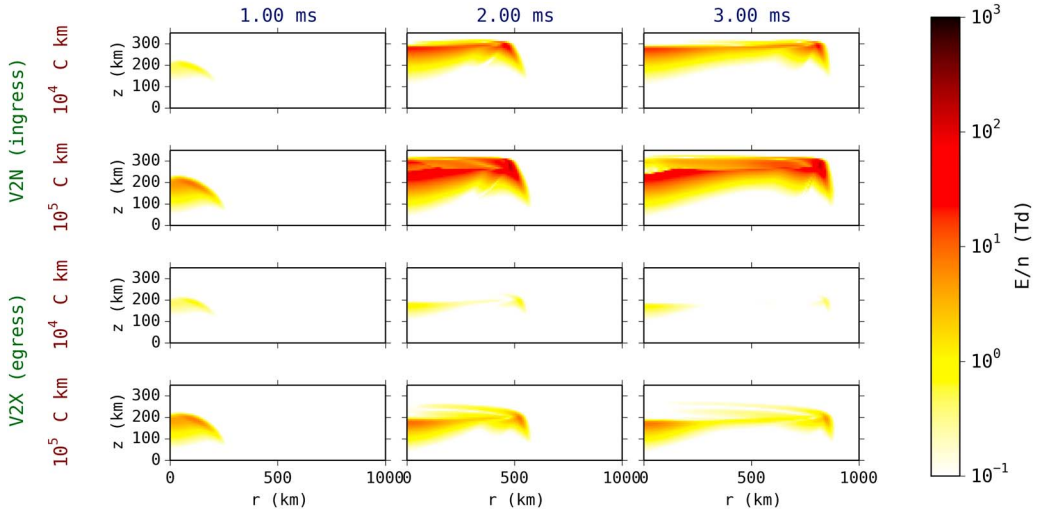

Figure 8. Reduced electric field E/n created in the atmosphere of Jupiter due to a lightning stroke. As for Saturn, we test two possible values for the charge moment change of the stroke, $M = 10^4$ C km and $M = 10^5$ C km and the two possible profiles of the electron density plotted in Figure 7. For each of the four resulting simulations, we show three snapshots of the reduced electric field.

the ionosphere starts at about 300 km, E/n may reach a few hundred Td if the charge moment change is 10^5 C km. The reduced electric field is much weaker in the case of profile V2X, where the ionosphere extends down to about 200 km: under those conditions the lightning EMP has a very modest influence on the atmosphere.

Once again, we can investigate the impact of lightning by looking at the electron density, photon emissions, and deposited energy a long time after the originating flash. Figure 9 represents these features after 20 ms. Also in this case the supporting information contains a plot of the net increase in electron density.

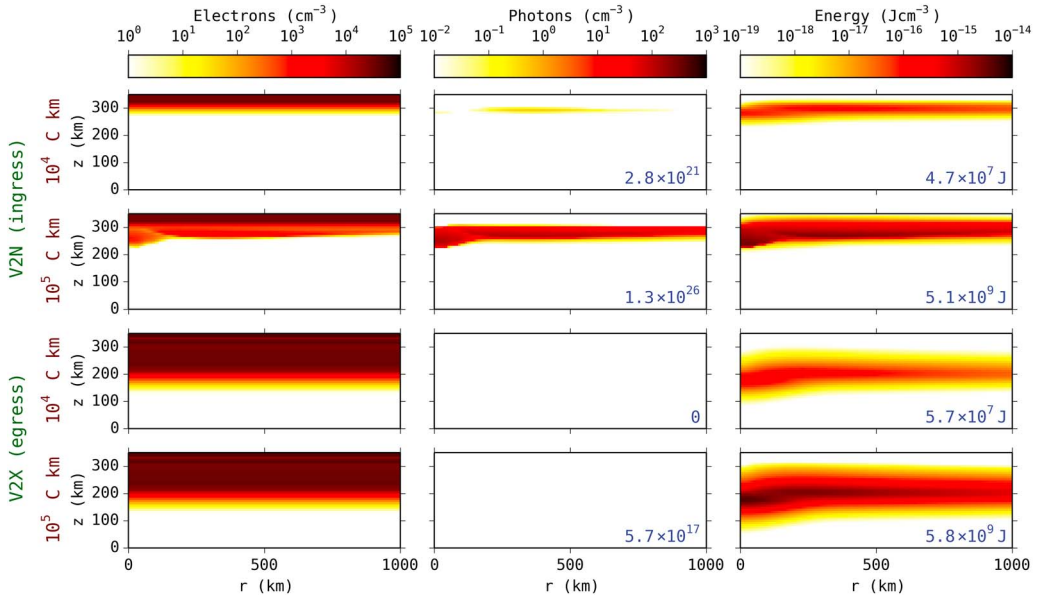

Figure 9. Effects of a lightning stroke on the upper atmosphere of Jupiter as reflected in the (left column) electron density, (middle column) photon emissions, and (right column) deposited energy density. The number in the lower right corner of the panels in the middle and right columns expresses, respectively, the total number of emitted photons and the total energy deposited in the upper atmosphere. In the supporting information we provide plots of the net increase in electron density. All the panels reflect the situation 20 ms after the stroke. Note that the total photon production for the V2X profile with a charge moment change $M = 10^4$ C km is below our numerical precision, and hence, it appears as 0.

The final electron density is in most cases barely affected by the stroke. Only with the high ionosphere of the V2N profile and a strong flash with $M = 10^5$ C km, the electron density is increased within a narrow layer below the ionosphere. That case is also the only one that produces a significant and eventually detectable photon emission, as plotted in the middle column of Figure 9. The total energy transferred to the upper atmosphere by Jovian lightning is about 10^7 J to 10^9 J per flash. As for Saturn, these energies may be enough to produce local effects but they are unlikely to have relevance in the global energy transport of Jupiter.

5. Discussion and Conclusions

Exploration of our solar system has taught us that atmospheric electricity is a common phenomenon outside Earth. In gaseous giants such as Jupiter and Saturn, lightning discharges are also much more energetic than on Earth. However, since their atmospheres have a lighter composition, typical distances are also longer and electromagnetic fields have to propagate a longer distance to reach a low gas density. Because the peak electric field of an electromagnetic pulse (EMP) decays only as the inverse of the distance from its source, at large distances it has a stronger impact on ionization and gas chemistry than the quasi-electrostatic (QE) field, which decays with the third power of distance. As we discussed in our previous work [*Dubrovin et al.*, 2014] the induction field, decaying as the square of the distance, dominates in the region vertically above the causating lightning.

As we have seen, this effect is particularly pronounced for Saturn. Under some circumstances, it is possible that lightning there induces very strong elves close to the lower ionosphere. Targeting these events for direct observation appears to be a daunting but not altogether impossible task.

One possibility would be to seek for signatures of high-altitude breakdown in lightning radio emissions, either in the thousands of SEDs detected by Cassini or in the Earth-based radio observations pioneered by *Zakharenko et al.* [2012]. However, the radio frequency fingerprint of elves on Saturn is yet to be understood. A strong elve increases the electron density in the lower ionosphere and therefore damps the outgoing wave; the precise frequency dependence of this damping and whether it will leave a clear mark in the spectrum is a possible subject of future studies.

Optical observations, even from a visiting spacecraft, are complicated by the emissions from the causative lighting stroke, which we estimate to be at least 10 times more intense than elves assuming perfect transmission. One option to discriminate both signals is to observe in the limb with a high spatial resolution. Also, the two signals have distinct spectra, with elves and other high-altitude emissions dominated by blue wavelengths of the Fulcher and continuum bands [*Dubrovin et al.*, 2010, 2014] and lightning emitting predominantly around the red H_α [*Borucki et al.*, 1985]. Therefore, a narrow wavelength filter can in principle be used to discriminate between them. However, the low detection rate of lightning by Cassini in Jupiter using a narrowband H_α filter [*Dyudina et al.*, 2004] as well as the signal observed in Saturn with a blue filter [*Dyudina et al.*, 2013] suggest that the spectrum of lightning in these planets is probably flatter than the one predicted by [*Borucki et al.*, 1985], possibly due to collisional broadening at pressures above 5 bar. Such a flat spectrum would hinder the distinction between both spectra.

A tantalizing possibility that deserves to be discussed is that the optical flashes detected in Saturn and Jupiter come from an intense elve instead of deep lightning strokes. This is specially suggestive given that, as mentioned above, daytime flashes were observed in Saturn with a blue filter. We believe, however, that this possibility contradicts the observed diameters and shapes of the flashes. *Dyudina et al.* [2010] reports diameters of about 200 km that according to the discussion in our section 4.1 would imply the existence of lightning discharges just about 100 km below the ionosphere. Also, since the Cassini images have a resolution of some tens of kilometers, they would be capable of seeing the central hole in the elve. An EMP interacting with the ionosphere may however produce different shapes if the axis of the originating discharge is heavily slanted with respect to the vertical. This is a possibility that deserves to be further investigated.

Our simulations show that the role of lightning-generated EMPs on the global energy transport of giant planets is negligible. However, EMPs may cause mesoscale effects such as a long-lived layer of ionization above active storms. The effects of such layers on the global chemistry of the planet are presently unclear.

Acknowledgments
The simulations in this paper used the GREMPY electromagnetic code, available at https://github.com/aluque/grempy. The input files used to run the simulations reported in the paper are available as supporting information. The full output can also be requested from the corresponding author. This work was supported by the Spanish Ministry of Economy and Competitiveness (MINECO) under projects AYA2011-29936-C05-02 and ESP2013-48032-C5-5-R and by the Junta de Andalucía, Proyecto de Excelencia FQM-5965. D.D. and Y.Y. were supported by the Israeli Ministry of Science, scholarship in Memory of Col. Ilan Ramon and by the Israeli Science Foundation grant 117/09.

Michael Liemohn thanks Ulyana Dyudina and another reviewer for their assistance in evaluating this paper.

References

Aplin, K. L. (2013), *Electrifying Atmospheres: Charging, Ionisation and Lightning in the Solar System and Beyond*, Springer, Dordrecht, Netherlands.
Astashkevich, S. A., and B. P. Lavrov (2002), Lifetimes of the electronic-vibrational-rotational states of hydrogen molecule (review), *Opt. Spectrosc.*, *92*, 818–850, doi:10.1134/1.1490020.
Baines, K. H., et al. (2007), Polar lightning and decadal-scale cloud variability on Jupiter, *Science*, *318*, 226–229, doi:10.1126/science.1147912.
Boeck, W. L., O. H. Vaughan Jr., R. Blakeslee, B. Vonnegut, and M. Brook (1992), Lightning induced brightening in the airglow layer, *Geophys. Res. Lett.*, *19*, 99–102, doi:10.1029/91GL03168.
Borucki, W. J., and C. P. McKay (1987), Optical efficiencies of lightning in planetary atmospheres, *Nature*, *328*, 509–510, doi:10.1038/328509a0.
Borucki, W. J., and M. A. Williams (1986), Lightning in the Jovian water cloud, *J. Geophys. Res.*, *91*, 9893–9903, doi:10.1029/JD091iD09p09893.
Borucki, W. J., R. L. McKenzie, C. P. McKay, N. D. Duong, and D. S. Boac (1985), Spectra of simulated lightning on Venus, Jupiter, and Titan, *Icarus*, *64*, 221–232, doi:10.1016/0019-1035(85)90087-9.
Bretagne, J., J. Godart, and V. Puech (1981), Time-resolved study of the H_2 continuum at low pressures, *J. Phys. B: At. Mol. Phys.*, *14*, L761, doi:10.1088/0022-3700/14/23/002.
Buckman, S. J., and A. Phelps (1985), *JILA Information Center Report No. 27*, Univ. of Colo., Boulder, Colo.
Cho, M., and M. J. Rycroft (2001), Non-uniform ionisation of the upper atmosphere due to the electromagnetic pulse from a horizontal lightning discharge, *J. Atmos. Sol. Terr. Phys.*, *63*, 559–580, doi:10.1016/S1364-6826(00)00235-2.
Cook, A. F., II, T. C. Duxbury, and G. E. Hunt (1979), First results on Jovian lightning, *Nature*, *280*, 794, doi:10.1038/280794a0.
Cumming, A., R. P. Butler, G. W. Marcy, S. S. Vogt, J. T. Wright, and D. A. Fischer (2008), The Keck Planet search: Detectability and the minimum mass and orbital period distribution of extrasolar planets, *Publ. Astron. Soc. Pac.*, *120*, 531–554, doi:10.1086/588487.
Desch, S. J., W. J. Borucki, C. T. Russell, and A. Bar-Nun (2002), Progress in planetary lightning, *Rep. Prog. Phys.*, *65*, 955–997, doi:10.1088/0034-4885/65/6/202.
Dubrovin, D., S. Nijdam, E. M. van Veldhuizen, U. Ebert, Y. Yair, and C. Price (2010), Sprite discharges on Venus and Jupiter-like planets: A laboratory investigation, *J. Geophys. Res.*, *115*, A00E34, doi:10.1029/2009JA014851.
Dubrovin, D., A. Luque, F. J. Gordillo-Vázquez, Y. Yair, F. C. Parra-Rojas, U. Ebert, and C. Price (2014), Impact of lightning on the lower ionosphere of Saturn and possible generation of halos and sprites, *Icarus*, *241*, 313–328, doi:10.1016/j.icarus.2014.06.025.
Dwyer, J. R., D. M. Smith, and S. A. Cummer (2012), High-energy atmospheric physics: Terrestrial gamma-ray flashes and related phenomena, *Space Sci. Rev.*, *173*, 133–196, doi:10.1007/s11214-012-9894-0.
Dyudina, U. A., A. P. Ingersoll, A. R. Vasavada, S. P. Ewald, and the Galileo SSI Team (2002), Monte Carlo radiative transfer modeling of lightning observed in Galileo images of Jupiter, *Icarus*, *160*, 336–349, doi:10.1006/icar.2002.6977.
Dyudina, U. A., A. D. Del Genio, A. P. Ingersoll, C. C. Porco, R. A. West, A. R. Vasavada, and J. M. Barbara (2004), Lightning on Jupiter observed in the H_α line by the Cassini imaging science subsystem, *Icarus*, *172*, 24–36, doi:10.1016/j.icarus.2004.07.014.
Dyudina, U. A., A. P. Ingersoll, S. P. Ewald, C. C. Porco, G. Fischer, W. S. Kurth, and R. A. West (2010), Detection of visible lightning on Saturn, *Geophys. Res. Lett.*, *37*, L09205, doi:10.1029/2010GL043188.
Dyudina, U. A., A. P. Ingersoll, S. P. Ewald, C. C. Porco, G. Fischer, and Y. Yair (2013), Saturn's visible lightning, its radio emissions, and the structure of the 2009–2011 lightning storms, *Icarus*, *226*, 1020–1037, doi:10.1016/j.icarus.2013.07.013.
Ebert, U., S. Nijdam, C. Li, A. Luque, T. Briels, and E. van Veldhuizen (2010), Review of recent results on streamer discharges and discussion of their relevance for sprites and lightning, *J. Geophys. Res.*, *115*, A00E43, doi:10.1029/2009JA014867.
Eshleman, V. R., G. L. Tyler, G. E. Wood, G. F. Lindal, J. D. Anderson, G. S. Levy, and T. A. Croft (1979), Radio science with Voyager at Jupiter—Initial Voyager 2 results and a Voyager 1 measure of the Io torus, *Science*, *206*, 959–962, doi:10.1126/science.206.4421.959.
Festou, M. C., and S. K. Atreya (1982), Voyager ultraviolet stellar occultation measurements of the composition and thermal profiles of the Saturnian upper atmosphere, *Geophys. Res. Lett.*, *9*, 1147–1150, doi:10.1029/GL009i010p01147.
Fischer, G., et al. (2006), Saturn lightning recorded by Cassini/RPWS in 2004, *Icarus*, *183*, 135–152, doi:10.1016/j.icarus.2006.02.010.
Fischer, G., D. A. Gurnett, W. S. Kurth, F. Akalin, P. Zarka, U. A. Dyudina, W. M. Farrell, and M. L. Kaiser (2008), Atmospheric electricity at Saturn, *Space Sci. Rev.*, *137*, 271–285, doi:10.1007/s11214-008-9370-z.
Franz, R. C., R. J. Nemzek, and J. R. Winckler (1990), Television image of a large upward electrical discharge above a thunderstorm system, *Science*, *249*, 48–51, doi:10.1126/science.249.4964.48.
Fukunishi, H., Y. Takahashi, M. Kubota, K. Sakanoi, U. S. Inan, and W. A. Lyons (1996), Elves: Lightning-induced transient luminous events in the lower ionosphere, *Geophys. Res. Lett.*, *23*, 2157–2160, doi:10.1029/96GL01979.
Galand, M., L. Moore, B. Charnay, I. Mueller-Wodarg, and M. Mendillo (2009), Solar primary and secondary ionization at Saturn, *J. Geophys. Res.*, *114*, A06313, doi:10.1029/2008JA013981.
Gordillo-Vázquez, F. J. (2008), Air plasma kinetics under the influence of sprites, *J. Phys. D: Appl. Phys.*, *41*(23), 234,016, doi:10.1088/0022-3727/41/23/234016.
Gordillo-Vázquez, F. J. (2010), Vibrational kinetics of air plasmas induced by sprites, *J. Geophys. Res.*, *115*, A00E25, doi:10.1029/2009JA014688.
Gordillo-Vázquez, F. J., and A. Luque (2010), Electrical conductivity in sprite streamer channels, *Geophys. Res. Lett.*, *37*, L16809, doi:10.1029/2010GL044349.
Gurnett, D. A., R. R. Shaw, R. R. Anderson, and W. S. Kurth (1979), Whistlers observed by Voyager 1—Detection of lightning on Jupiter, *Geophys. Res. Lett.*, *6*, 511–514, doi:10.1029/GL006i006p00511.
Gurnett, D. A., W. S. Kurth, I. H. Cairns, and L. J. Granroth (1990), Whistlers in Neptune's magnetosphere—Evidence of atmospheric lightning, *J. Geophys. Res.*, *95*, 20,967–20,976, doi:10.1029/JA095iA12p20967.
Hagelaar, G. J. M., and L. C. Pitchford (2005), Solving the Boltzmann equation to obtain electron transport coefficients and rate coefficients for fluid models, *Plasma Sources Sci. Technol.*, *14*, 722, doi:10.1088/0963-0252/14/4/011.
Haldoupis, C., M. Cohen, E. Arnone, B. Cotts, and S. Dietrich (2013), The VLF fingerprint of elves: Step-like and long-recovery early VLF perturbations caused by powerful ±CG lightning EM pulses, *J. Geophys. Res. Space Physics*, *118*, 5392–5402, doi:10.1002/jgra.50489.
Helling, C., M. Jardine, and F. Mokler (2011), Ionization in atmospheres of Brown Dwarfs and extrasolar planets. II. Dust-induced collisional ionization, *Astrophys. J.*, *737*, 38, doi:10.1088/0004-637X/737/1/38.
Hinson, D. P., F. M. Flasar, A. J. Kliore, P. J. Schinder, J. D. Twicken, and R. G. Herrera (1997), Jupiter's ionosphere: Results from the first Galileo radio occultation experiment, *Geophys. Res. Lett.*, *24*, 2107–2110, doi:10.1029/97GL01608.
Hinson, D. P., J. D. Twicken, and E. T. Karayel (1998), Jupiter's ionosphere: New results from Voyager 2 radio occultation measurements, *J. Geophys. Res.*, *103*, 9505–9520, doi:10.1029/97JA03689.

Howard, A. W. (2013), Observed properties of extrasolar planets, *Science*, *340*, 572–576, doi:10.1126/science.1233545.
Inan, U., and R. Marshall (2011), *Numerical Electromagnetics: The FDTD Method*, Cambridge Univ. Press, New York.
Inan, U. S., T. F. Bell, and J. V. Rodriguez (1991), Heating and ionization of the lower ionosphere by lightning, *Geophys. Res. Lett.*, *18*, 705–708, doi:10.1029/91GL00364.
Inan, U. S., S. A. Cummer, and R. A. Marshall (2010), A survey of ELF and VLF research on lightning-ionosphere interactions and causative discharges, *J. Geophys. Res.*, *115*, A00E36, doi:10.1029/2009JA014775.
Jackson, J. (1975), *Classical Electrodynamics*, John Wiley, New York.
Kaiser, M. L., M. D. Desch, W. M. Farrell, and P. Zarka (1991), Restrictions on the characteristics of Neptunian lightning, *J. Geophys. Res.*, *96*(S01), 19043–19047.
Kuo, C. L., A. B. Chen, J. K. Chou, L. Y. Tsai, R. R. Hsu, H. T. Su, H. U. Frey, S. B. Mende, Y. Takahashi, and L. C. Lee (2008), Radiative emission and energy deposition in transient luminous events, *J. Phys. D: Appl. Phys.*, *41*(23), 234,014, doi:10.1088/0022-3727/41/23/234014.
Lee, J. H., and D. Kalluri (1999), Three-dimensional FDTD simulation of electromagnetic wave transformation in a dynamic inhomogeneous magnetized plasma, *IEEE Trans. Antennas Propag.*, *47*(7), 1146–1151, doi:10.1109/8.785745.
Li, L., et al. (2010), Saturn's emitted power, *J. Geophys. Res.*, *115*, E11002, doi:10.1029/2010JE003631.
Little, B., C. D. Anger, A. P. Ingersoll, A. R. Vasavada, D. A. Senske, H. H. Breneman, W. J. Borucki, and The Galileo SSI Team (1999), Galileo images of lightning on Jupiter, *Icarus*, *142*, 306–323, doi:10.1006/icar.1999.6195.
Luque, A. (2014), Relativistic runaway ionization fronts, *Phys. Rev. Lett.*, *112*(4), 45,003, doi:10.1103/PhysRevLett.112.045003.
Luque, A., and U. Ebert (2009), Emergence of sprite streamers from screening-ionization waves in the lower ionosphere, *Nat. Geosci.*, *2*, 757–760, doi:10.1038/ngeo662.
Luque, A., and U. Ebert (2012), Density models for streamer discharges: Beyond cylindrical symmetry and homogeneous media, *J. Comput. Phys.*, *231*, 904–918, doi:10.1016/j.jcp.2011.04.019.
Luque, A., V. Ratushnaya, and U. Ebert (2008), Positive and negative streamers in ambient air: Modelling evolution and velocities, *J. Phys. D: Appl. Phys.*, *41*(23), 234,005, doi:10.1088/0022-3727/41/23/234005.
Marshall, R. A. (2012), An improved model of the lightning electromagnetic field interaction with the *D* region ionosphere, *J. Geophys. Res.*, *117*, A03316, doi:10.1029/2011JA017408.
Marshall, R. A., U. S. Inan, and V. S. Glukhov (2010), Elves and associated electron density changes due to cloud-to-ground and in-cloud lightning discharges, *J. Geophys. Res.*, *115*, A00E17, doi:10.1029/2009JA014469.
Moore, L. E., M. Mendillo, I. C. F. Müller-Wodarg, and D. L. Murr (2004), Modeling of global variations and ring shadowing in Saturn's ionosphere, *Icarus*, *172*, 503–520, doi:10.1016/j.icarus.2004.07.007.
Moses, J. I., B. Bézard, E. Lellouch, G. R. Gladstone, H. Feuchtgruber, and M. Allen (2000), Photochemistry of Saturn's atmosphere. I. Hydrocarbon chemistry and comparisons with ISO observations, *Icarus*, *143*, 244–298, doi:10.1006/icar.1999.6270.
Parra-Rojas, F. C., A. Luque, and F. J. Gordillo-Vázquez (2013), Chemical and electrical impact of lightning on the Earth mesosphere: The case of sprite halos, *J. Geophys. Res. Space Physics*, *118*, 5190–5214, doi:10.1002/jgra.50449.
Pasko, V. P., Y. Yair, and C.-L. Kuo (2012), Lightning related transient luminous events at high altitude in the Earth's atmosphere: Phenomenology, mechanisms and effects, *Space Sci. Rev.*, *168*, 475–516, doi:10.1007/s11214-011-9813-9.
Porco, C. C., et al. (2004), Cassini imaging science: Instrument characteristics and anticipated scientific investigations at Saturn, *Space Sci. Rev.*, *115*, 363–497, doi:10.1007/s11214-004-1456-7.
Rinnert, K., and L. J. Lanzerotti (1998), Radio wave propagation below the Jovian ionosphere, *J. Geophys. Res.*, *103*, 22,993–22,999, doi:10.1029/98JE01968.
Rowland, H. L., R. F. Fernsler, and P. A. Bernhardt (1996), Breakdown of the neutral atmosphere in the *D* region due to lightning driven electromagnetic pulses, *J. Geophys. Res.*, *101*, 7935–7945, doi:10.1029/95JA03519.
Shao, X. M., and P. R. Krehbiel (1996), The spatial and temporal development of intracloud lightning, *J. Geophys. Res.*, *101*, 26,641–26,668, doi:10.1029/96JD01803.
Shao, X.-M., E. H. Lay, and A. R. Jacobson (2013), Reduction of electron density in the night-time lower ionosphere in response to a thunderstorm, *Nat. Geosci.*, *6*, 29–33, doi:10.1038/ngeo1668.
Showman, A. (2003), Planetary atmospheres: Jupiter and the outer planets, in *Encyclopedia of Atmospheric Sciences*, edited by J. R. Holton, pp. 1730–1745, Academic Press, Oxford, U. K., doi:10.1016/B0-12-227090-8/00314-6.
Taranenko, Y. N., U. S. Inan, and T. F. Bell (1993a), The interaction with the lower ionosphere of electromagnetic pulses from lightning: Excitation of optical emissions, *Geophys. Res. Lett.*, *20*, 2675–2678, doi:10.1029/93GL02838.
Taranenko, Y. N., U. S. Inan, and T. F. Bell (1993b), Interaction with the lower ionosphere of electromagnetic pulses from lightning—Heating, attachment, and ionization, *Geophys. Res. Lett.*, *20*, 1539–1542, doi:10.1029/93GL01696.
United States Committee on Extension to the Standard Atmosphere (1976), *US Standard Atmosphere*, U. S. Government Printing Office, Washington, D. C.
Veronis, G., V. P. Pasko, and U. S. Inan (1999), Characteristics of mesospheric optical emissions produced by lighting discharges, *J. Geophys. Res.*, *104*, 12,645–12,656, doi:10.1029/1999JA900129.
Warwick, J. W., et al. (1981), Planetary radio astronomy observations from Voyager 1 near Saturn, *Science*, *212*, 239–243, doi:10.1126/science.212.4491.239.
Wilson, C. T. R. (1925), The electric field of a thundercloud and some of its effects, *Proc. Phys. Soc. London*, *37*, 32D, doi:10.1088/1478-7814/37/1/314.
Yair, Y. (2012), New results on planetary lightning, *Adv. Space Res.*, *50*, 293–310, doi:10.1016/j.asr.2012.04.013.
Yair, Y., Z. Levin, and S. Tzivion (1995), Lightning generation in a Jovian thundercloud: Results from an axisymmetric numerical cloud model., *Icarus*, *115*, 421–432, doi:10.1006/icar.1995.1108.
Yair, Y., G. Fischer, F. Simões, N. Renno, and P. Zarka (2008), Updated review of planetary atmospheric electricity, *Space Sci. Rev.*, *137*, 29–49, doi:10.1007/s11214-008-9349-9.
Yair, Y., Y. Takahashi, R. Yaniv, U. Ebert, and Y. Goto (2009), A study of the possibility of sprites in the atmospheres of other planets, *J. Geophys. Res.*, *114*, E09002, doi:10.1029/2008JE003311.
Yee, K. (1966), Numerical solution of initial boundary value problems involving Maxwell's equations in isotropic media, *IEEE Trans. Antennas Propag.*, *14*(3), 302–307, doi:10.1109/TAP.1966.1138693.
Yelle, R. V., and S. Miller (2007), Jupiter's thermosphere and ionosphere, in *Jupiter: The Planet, Satellites and Magnetosphere*, edited by F. Bagenal et al., Cambridge Univ. Press, Cambridge, U. K.
Zakharenko, V., et al. (2012), Ground-based and spacecraft observations of lightning activity on Saturn, *Planet. Space Sci.*, *61*, 53–59, doi:10.1016/j.pss.2011.07.021.
Zarka, P., and B. M. Pedersen (1986), Radio detection of Uranian lightning by Voyager 2, *Nature*, *323*, 605–608, doi:10.1038/323605a0.